The Journal of Chemical Physics

RESEARCH ARTICLE | FEBRUARY 09 2024

Weak second-order quantum state diffusion unraveling of the Lindblad master equation FREE

Sayak Adhikari ; Roi Baer

J. Chem. Phys. 160, 064107 (2024)
https://doi.org/10.1063/5.0191947

The Journal of Chemical Physics ARTICLE pubs.aip.org/aip/jcp

Weak second-order quantum state diffusion unraveling of the Lindblad master equation

Cite as: J. Chem. Phys. 160, 064107 (2024); doi: 10.1063/5.0191947
Submitted: 17 December 2023 • Accepted: 18 January 2024 •
Published Online: 9 February 2024

Sayak Adhikari and Roi Baer[a)]

AFFILIATIONS

Fritz Haber Center for Molecular Dynamics and Institute of Chemistry, The Hebrew University of Jerusalem, Jerusalem 9190401, Israel

[a)]Author to whom correspondence should be addressed: roi.baer@mail.huji.ac.il

ABSTRACT

Simulating mixed-state evolution in open quantum systems is crucial for various chemical physics, quantum optics, and computer science applications. These simulations typically follow the Lindblad master equation dynamics. An alternative approach known as quantum state diffusion unraveling is based on the trajectories of pure states generated by random wave functions, which evolve according to a nonlinear Itô–Schrödinger equation (ISE). This study introduces weak first-order and second-order solvers for the ISE based on directly applying the Itô–Taylor expansion with exact derivatives in the interaction picture. We tested the method on free and driven Morse oscillators coupled to a thermal environment and found that both orders allowed practical estimation with a few dozen iterations. The variance was relatively small compared to the linear unraveling and did not grow with time. The second-order solver delivers a much higher accuracy and stability with bigger time steps than the first-order scheme, with a small additional workload. However, the second-order algorithm has quadratic complexity with the number of Lindblad operators as opposed to the linear complexity of the first-order algorithm.

I. INTRODUCTION

When a physical system in a pure quantum state is brought to interact weakly with a macroscopic thermal environment, it changes its energy and chemical composition. At the same time, it gradually loses its "quantumness" or, more technically, its phase coherence. Ultimately, the system's state resembles that drawn randomly from the Gibbs ensemble at the environment's temperature and chemical potentials. All quantum systems interact with the environment. Therefore, techniques to simulate decoherence and decay processes are vital for developing quantum technologies and studying chemical processes in solutions and condensed matter.[1–17]

The pure quantum state of an open system is not known with certainty, and thus, we consider it a random mixture of pure states. The density operator ρ is the mathematical object that best describes this mixture, enabling the calculation of probabilities of outcomes of measurements. Even when the initial mixture $\rho(0)$ is known, the density operator $\rho(t)$ changes over time. The Redfield master equation[1,3,18–21] is one way to approximate this evolution, but it sometimes creates mixtures with negative probabilities. Lindblad's master equation[13,22–25] is an augmented form of Redfield's equation, guaranteeing the density operator's positivity. It is a quantum Liouville-like equation but includes additional terms, relying on Lindblad operators, to represent the dressed system–environment interactions.

The density operator of the Lindblad equation can be modeled by stochastic processes collectively called "quantum unraveling models."[5,26,27] They provide recipes for generating a random time-dependent normalized pure state $|\psi(t)\rangle$ for which the expected value of the projector, $\mathbb{E}[|\psi(t)\rangle\langle\psi(t)|]$, is equal to the Lindblad density operator $\rho(t)$. One type of unraveling is the Monte-Carlo wave function approach,[28–30] also known as the "quantum jumps model," where the Lindblad operators create abrupt "jumps" in quantum space. A second approach to unraveling is the "quantum state diffusion model,"[31] which involves a norm-conserving (but not unitary) time-dependent stochastic Itô–Schrödinger equation (ISE) for $|\psi(t)\rangle$. The ISE contains drift (evolution) and diffusion (fluctuation) terms. The quantum jump and quantum state diffusion models yield different trajectories. The former evolves non-continuously. At the same time, the latter is continuous but non-differentiable in time.

One advantage of basing numerical simulations on the quantum state diffusion model is the availability of well-established high-order techniques for solving stochastic differential equations (SDEs).[5,32–34] In the present contribution, we deploy a simple approach based on the exact derivatives in the interaction picture, an Itô–Taylor expansion for weak second-order solutions. The method is stable and allows for high accuracy and slight variance.

II. WEAK SECOND-ORDER QUANTUM STATE DIFFUSION UNRAVELING

A. Comments on notation

Before we start the detailed theory, here are several comments concerning the notation in this paper:

1. The time dimension of any quantity can be read off from its superscripts or subscripts: a subscript 0 adds a dimension of $time^{-1}$ and a superscript 0 attributes a dimension of $time^{+1}$. Thus, the Hamiltonian $\mathcal{H}_0$ has the dimension of inverse time, while the symbol I^0 has the dimension of time. A Greek subscript attributes an additional factor of $time^{-1/2}$, and a Greek superscript attributes an additional factor of $time^{1/2}$. Thus, the symbol I^α has the dimension of $time^{1/2}$, while $I_{\alpha\beta}$ has the dimension of $time^{-1}$. The Kronecker delta δ^β_α is dimensionless. Furthermore, the symbols I^0_α and $I^{\alpha\beta}_\gamma$ have the dimension of $time^{1/2}$, while $I^{0\alpha}$ has the dimensions of $time^{3/2}$. These conventions help ascertain that the different time orders we use in our analytical developments are consistent (i.e., that we do not add quantities with different time dimensions).
2. The indices α and α' going from $1,\ldots,N_L$ denote one of the N_L Lindblad operators. When two quantities indexed with α are multiplied in an expression, a summation over α from 1 to N_L is assumed and we omit the explicit $\sum_{\alpha=1}^{N_L}$ notation (this is the so-called Einstein convention). If the index is decorated by a dot $\dot\alpha$, then no such summation is implied.
3. In the following, we introduce a "0" operator, in addition to the Lindblad operators. Unlike the α and α' indices discussed above going from $1,\ldots,N_L$, we also use the β and β' indices to enumerate operators and quantities that range from 0 to N_L. Similar to the case with α, when two quantities indexed with β are multiplied in an expression, a summation over β is assumed and we omit the explicit $\sum_{\beta=0}^{N_L}$ notation. If the index is decorated by a dot $\dot\beta$, then no such summation is implied.

B. Quantum state diffusion unraveling

The Lindblad equation

$$\dot\rho(t) = -i[\mathcal{H}_0 + \theta(t)\mathcal{V}_0, \rho] + \mathscr{D}_0\rho, \tag{1}$$

together with the initial condition $\rho(0)$, determines $\rho(t)$ for all time $t > 0$. It contains unitary terms dependent on $\mathcal{H}_0$, an effective Hamiltonian operator, and $\theta(t)\mathcal{V}_0$, a driving force with $\theta(t)$, a dimensionless real time-dependent envelop with time derivative $\theta_0(t) \equiv \dot\theta(t)$. It also contains dissipative terms as follows:[13,24,25,31]

$$\mathscr{D}_0\rho \equiv \left[\mathcal{L}_\alpha\rho, \mathcal{L}^\dagger_\alpha\right] + \left[\mathcal{L}_\alpha, \rho\mathcal{L}^\dagger_\alpha\right], \tag{2}$$

defined in terms of the Lindblad operators $\mathcal{L}_\alpha$, $\alpha = 1,\ldots,N_L$. Atomic units are used here ($\hbar = 1$, $m_e = 1$), so the energy and inverse time units are identical. Accordingly, $\mathcal{L}_\alpha$ have the dimension of $time^{-1/2}$.

Evolving the mixed-state density operator $\rho(t)$ using Eq. (1) can be numerically expensive when systems are large. A possible simplification can be achieved by the unraveling procedure, which evolves a pure random state $|\psi(t)\rangle$ in such a way that $\mathbb{E}[|\psi(t)\rangle\langle\psi(t)|] = \rho(t)$. In quantum state diffusion, unraveling $|\psi(t)\rangle$ is obtained from the following Itô–Schrödinger equation (ISE):[31]

$$|d\psi\rangle = -i\mathcal{H}_0|\psi\rangle dw^0 + \Lambda_\beta|\psi\rangle dw^\beta, \tag{3}$$

starting from a random ket $|\psi(0)\rangle$ for which $\mathbb{E}[|\psi(0)\rangle\langle\psi(0)|] = \rho(0)$. In Eq. (3),

$$\Lambda_\alpha \equiv \mathcal{L}_\alpha - \langle\mathcal{L}_\alpha\rangle,$$
$$\Lambda_0 \equiv -i\theta(t)\mathcal{V}_0(t) + \left(2\left\langle\mathcal{L}^\dagger_\alpha\right\rangle\mathcal{L}_\alpha - \mathcal{L}^\dagger_\alpha\mathcal{L}_\alpha - \left\langle\mathcal{L}^\dagger_\alpha\right\rangle\langle\mathcal{L}_\alpha\rangle\right),$$

and

$$\langle\mathcal{L}_\alpha\rangle \equiv \frac{\langle\psi|\mathcal{L}_\alpha|\psi\rangle}{\langle\psi|\psi\rangle}. \tag{4}$$

Notice that $\langle\Lambda_\alpha\rangle = 0$ (for $\alpha = 1,\ldots,N_L$). In Eq. (3), $dw^0 = dt$ is the time-step, while dw^α, $\alpha = 1, 2, \ldots N_L$, are independent complex Wiener processes, with real $\Re[dw^\alpha]$ and imaginary $\Im[dw^\alpha]$ parts, each of which is an independent real Wiener process with zero expected value and a variance equal to dt. As is common in the stochastic differential equations literature, we omit the expected value symbol $\mathbb{E}$ from differentials; hence, we are lead to the following variances for dw^α:

$$\left(dw^\alpha\right)^2 = \left(dw^{\alpha*}\right)^2 = 0, \quad \left|dw^\alpha\right|^2 = 2dt. \tag{5}$$

Note that dw^α are also independent of $|\psi\rangle$. Note that the differential $d\langle\psi|\psi\rangle \equiv \langle d\psi|\psi\rangle + \langle\psi|d\psi\rangle + \langle d\psi|d\psi\rangle$ vanishes when evaluated using Eqs. (3)–(5). Hence, $\langle\psi|\psi\rangle$ is a constant of motion, separately for each trajectory.

C. Weak first-order and second-order propagators

The first step in providing a solution to the ISE is to move to the interaction picture, defining $|\phi(t)\rangle \equiv e^{i\mathcal{H}_0 t}|\psi(t)\rangle$ and, for any operator $\mathcal{Y}$, $\mathcal{Y}(t) \equiv e^{i\mathcal{H}_0 t}\mathcal{Y}e^{-i\mathcal{H}_0 t}$. The ISE of Eq. (3) becomes

$$d|\phi\rangle = dw^\beta\Lambda_\beta(t)|\phi\rangle, \tag{6}$$

where

$$\Lambda_\alpha(t) \equiv \mathcal{L}_\alpha(t) - \langle\mathcal{L}_\alpha(t)\rangle, \tag{7}$$

and note that our definition of the expectation value

$$\langle\mathcal{L}_\alpha(t)\rangle \equiv \frac{\langle\psi(t)|\mathcal{L}_\alpha|\psi(t)\rangle}{\langle\psi(t)|\psi(t)\rangle} = \frac{\langle\phi(t)|\mathcal{L}_\alpha(t)|\phi(t)\rangle}{\langle\phi(t)|\phi(t)\rangle},$$

which includes division by the norm and is thus different from some other applications.[33] Formally, there is no need to divide by the

norm since one can choose the initial norm as 1 and it is preserved. However, in practice, the norm is never perfectly preserved, so this division is not a trivial change and we found that division by the norm leads to a more stable numerical behavior.

For developing the numerical scheme, we divide time $t \in [0, T_f]$, where T_f is the final time, into N_T discrete small temporal segments $\Delta T = T_f/N_T$ and designate $t_{n+1} = t_0 + n\Delta T$, $n = 1, 2, \ldots, N_T$. Using the notation $|\Phi\rangle \equiv |\phi(t_n)\rangle$, the change in the evolving ket during the nth time step, $|\Delta\Phi\rangle \equiv |\phi(t_{n+1})\rangle - |\Phi\rangle$, is expressed as a stochastic integral over $d|\phi\rangle$, which gives the following equation:

$$|\Delta\Phi\rangle = \int_{t_n}^{t_n+\Delta T} \Lambda_\beta(\tau)|\phi(\tau)\rangle dw_\tau^\beta. \tag{8}$$

We strive for an approximation of this integral, which allows an exact solution of the ISE in the limit of $N_T \to \infty$ and, accordingly, $\Delta T \to 0$. Our analysis follows closely that found in the classical literature on numerical solutions of real SDEs.[35,36] Our contribution is the adaptation of the theory to Eq. (6), including the use of complex Wiener processes and exact analytical derivatives therein. We also contribute a simplified notation scheme.

The change in the wave function is provided in terms of first-order and second-order contributions, $|\Delta\Phi\rangle \approx \left|\Delta^{(1)}\Phi\right\rangle + \left|\Delta^{(2)}\Phi\right\rangle$. The first-order term is obtained by approximating $\Lambda_\beta(\tau)|\phi(\tau)\rangle$ as $|\beta\rangle \equiv \Lambda_\beta(t_n)|\Phi\rangle$ for $\tau \in [t_n, t_n + \Delta T]$. This gives

$$\left|\Delta^{(1)}\Phi\right\rangle = I^\beta|\beta\rangle, \tag{9}$$

where $I^\alpha = \int_{t_n}^{t_n+\Delta T} dw^\alpha$, $\alpha = 1, \ldots, N_L$, are Itô integrals presented in Table I and $I^0 = \Delta T$. In the numerical calculations, we use the model for the complex stochastic Itô integrals given in the last column of the table.

We use the Itô–Taylor expansion to the lowest order for the second-order correction. For this, we introduce a notation in which all quantities are first written as functions of a ket $|x\rangle$ and a (different) bra $\langle y|$, and then, we take separate derivatives with respect to them and only after that do we set $|x\rangle = |\Phi\rangle$ and $\langle y| = \langle\Phi|$. In the supplementary material, we provide a detailed explanation of the results presented here. We define for $\alpha = 1, \ldots, N_L$ the ℓ-functions of $|x\rangle$, $\langle y|$, and the time t,

$$\ell_\alpha(|x\rangle, \langle y|, t) \equiv \frac{\langle y|\mathcal{L}_\alpha(t)|x\rangle}{\langle y|x\rangle}$$

and

$$\ell_\alpha^*(|x\rangle, \langle y|, t) \equiv \frac{\langle y|\mathcal{L}_\alpha^\dagger(t)|x\rangle}{\langle y|x\rangle},$$

which when evaluated at Φ, become the expectation values of the Lindblad operators,

$$(\ell_\alpha(|x\rangle, \langle y|, t))_\Phi \equiv \ell_\alpha(|\Phi\rangle, \langle\Phi|, t) = \langle\mathcal{L}_\alpha(t)\rangle,$$
$$\left(\ell_\alpha^*(|x\rangle, \langle y|, t)\right)_\Phi \equiv \ell_\alpha^*(|\Phi\rangle, \langle\Phi|, t) = \left\langle\mathcal{L}_\alpha^\dagger(t)\right\rangle.$$

The derivative of $\ell_\alpha(|x\rangle, \langle y|, t)$ with respect to the bra $\langle y|$ results in a ket,

$$\left|\frac{\partial}{\partial\langle y|}\ell_\alpha(|x\rangle, \langle y|, t)\right\rangle = \frac{(\mathcal{L}_\alpha(t) - \ell_\alpha(|x\rangle, \langle y|, t))|x\rangle}{\langle y|x\rangle} \equiv \frac{|\lambda_\alpha(|x\rangle, \langle y|, t))}{\langle y|x\rangle}, \tag{10}$$

which is orthogonal to $|y\rangle$,

$$\langle y|\lambda_\alpha\rangle = 0.$$

Similarly, the derivative with respect to the ket $|x\rangle$ results in a bra,

$$\left\langle\frac{\partial}{\partial|x\rangle}\ell_\alpha(|x\rangle, \langle y|, t)\right| = \frac{\langle y|(\mathcal{L}_\alpha(t) - \ell_\alpha(|x\rangle, \langle y|, t))}{\langle y|x\rangle} \equiv \langle\mu_\alpha(|x\rangle, \langle y|, t)|,$$

TABLE I. The definition of the stochastic Itô integrals used in Eqs. (9)–(12), where t_n are the propagation time steps, with $t_{n+1} - t_n = \Delta T$, and $\alpha, \alpha', \alpha'', \alpha''' = 1, \ldots, N_L$ are Lindblad indices, and $\alpha^* \equiv \alpha + N_L$. All the integrals have zero expected value and covariance described in the table. The integrals I^0 and I^{00} are deterministic and equal to ΔT and $\frac{\Delta T^2}{2}$, respectively. The last column for each integral gives a model depending on $4 \times N_L$ independent complex random variables m^α ($\alpha = 1, \ldots, N_L$, $m = a, b, c, d$), distributed with $\mathbb{E}[m^\alpha] = 0$, $\mathbb{E}\left[m^\alpha m'^{\alpha'}\right] = 0$, and $\mathbb{E}\left[m^{\alpha*} m'^{\alpha'}\right] = 2\Delta T\delta_{\alpha\alpha'}\delta_{mm'}$. For each time interval $t_n \to t_{n+1}$, a new uncorrelated set of such random variables is used.

Integral	$I^{\alpha'*}$	$I^{\alpha'*0}$	$I^{0\alpha'*}$	$I^{\alpha''*\alpha'''*}$	$I^{\alpha''\alpha'''*}$	Model
$I^\alpha \equiv \int_0^{\Delta T} dw_\tau^\alpha$	$\delta_{\alpha'}^\alpha 2\Delta T$	$\delta_{\alpha'}^\alpha \Delta T^2$	$\delta_{\alpha'}^\alpha \Delta T^2$	0	0	a^α
$I^{\alpha 0} \equiv \int_0^{\Delta T}\int_0^\tau dw_{\tau'}^\alpha d\tau$	$\delta_{\alpha'}^\alpha \Delta T^2$	$\delta_{\alpha'}^\alpha \frac{2\Delta T^3}{3}$	$\delta_{\alpha'}^\alpha \frac{\Delta T^3}{3}$	0	0	$\left(a^\alpha + \frac{1}{\sqrt{3}}b^\alpha\right)\frac{\Delta T}{2}$
$I^{0\alpha} \equiv \int_0^{\Delta T}(\tau - t_n)dw_\tau^\alpha$	$\delta_{\alpha'}^\alpha \Delta T^2$	$\delta_{\alpha'}^\alpha \frac{\Delta T^3}{3}$	$\delta_{\alpha'}^\alpha \frac{2\Delta T^3}{3}$	0	0	$\left(a^\alpha - \frac{1}{\sqrt{3}}b^\alpha\right)\frac{\Delta T}{2}$
$I^{\alpha\alpha'} \equiv \int_0^{\Delta T} dw_\tau^\alpha \int_0^\tau dw_{\tau'}^{\alpha'}$	0	0	0	$\delta_{\alpha''}^\alpha\delta_{\alpha'}^{\alpha'''} 2\Delta T^2$	0	$\frac{1}{\sqrt{2}}c^\alpha d^{\alpha'}$
$I^{\alpha*\alpha'} \equiv \int_0^{\Delta T} dw_\tau^{\alpha*}\int_0^\tau dw_{\tau'}^{\alpha'}$	0	0	0	0	$\delta_{\alpha''}^\alpha\delta_{\alpha'}^{\alpha'''} 2\Delta T^2$	$\frac{1}{\sqrt{2}}(c^\alpha)^* d^{\alpha'}$

which is orthogonal to $|x\rangle$,

$$\langle \mu_\alpha | x \rangle = 0.$$

We extend the definition of the "λ-kets," by adding a "zero" subscript,

$$|\lambda_0(|x\rangle,\langle y|,t)\rangle \equiv -i\mathcal{V}_0(t)\theta(t)|x\rangle + \Big(2\ell_\alpha^*(|x\rangle,\langle y|,t)\,\mathcal{L}_\alpha - \mathcal{L}_\alpha^\dagger\mathcal{L}_\alpha - \ell_\alpha(|x\rangle,\langle y|,t)\ell_\alpha^*(|x\rangle,\langle y|,t)\Big)|x\rangle. \tag{11}$$

When evaluated at Φ, for $\beta = 0,\ldots,N_L$, we have the following equation:

$$\big|\lambda_\beta(|x\rangle,\langle y|,t)\big\rangle_{\Phi,t_n} \equiv \Lambda_\beta|\Phi\rangle \equiv |\beta\rangle.$$

With these definitions, the second-order correction is given in terms of λ-kets, t, $|x\rangle$, $\langle y|$ first derivatives, and the $|x\rangle\langle y|$ mixed derivatives as follows:

$$\begin{aligned}\big|\Delta^{(2)}\Phi\big\rangle = {} & I^{0\beta}\Big(\frac{\partial}{\partial t}|\lambda_\beta\rangle\Big)_{\Phi,t_n} + \underbrace{I^{\beta\beta'}\Big(\frac{\partial}{\partial|x\rangle}|\lambda_{\beta'}\rangle\Big)_{\Phi,t_n}|\beta\rangle}_{'X'} \\ & + \underbrace{I^{\beta*\beta'}\langle\beta|\Big(\frac{\partial}{\partial\langle y|}|\lambda_{\beta'}\rangle\Big)_{\Phi,t_n}}_{'Y'} \\ & + \underbrace{2I^{0\beta}\langle\alpha|\Big(\frac{\partial^2}{\partial|x\rangle\partial\langle y|}|\lambda_\beta\rangle\Big)_{\Phi,t_n}|\alpha\rangle}_{'XY'},\end{aligned} \tag{12}$$

where $I^{\beta\beta'}$ ($\beta = 0,\ldots,N_L$ and $\beta' = 0,\ldots,N_L$) are the Itô integrals presented in Table I.

The derivatives in the expression for $\big|\Delta\Phi^{(2)}\big\rangle$ are

$$\begin{aligned}\Big(\frac{\partial}{\partial t}|\lambda_\alpha\rangle\Big)_{\Phi,t_n} &= i([\mathcal{H}_0,\Lambda_\alpha] - \langle[\mathcal{H}_0,\Lambda_\alpha]\rangle)|\Phi\rangle, \\ \Big(\frac{\partial}{\partial t}|\lambda_0\rangle\Big)_{\Phi,t_n} &= (\theta(t_n)[\mathcal{H}_0,\mathcal{V}_0] - i\theta_0(t_n)\mathcal{V}_0)|\Phi\rangle \\ &\quad + i\Big(2\Big\langle\Big[\mathcal{H}_0,\Lambda_\alpha^\dagger\Big]\Big\rangle\Lambda_\alpha - \Big[\mathcal{H}_0,\Lambda_\alpha^\dagger\Lambda_\alpha\Big]\Big)|\Phi\rangle \\ &\quad + i\Big\langle\mathcal{L}_\alpha^\dagger\Big\rangle([\mathcal{H}_0,\Lambda_\alpha] - \langle[\mathcal{H}_0,\Lambda_\alpha]\rangle)|\Phi\rangle.\end{aligned}$$

Next, using the notations $|\beta\rangle \equiv \Lambda_\beta|\Phi\rangle$, $|\alpha\beta\rangle \equiv \Lambda_\alpha\Lambda_\beta|\Phi\rangle$, etc., the x-derivatives are

$$\begin{aligned}\Big(\frac{\partial}{\partial|x\rangle}|\lambda_\alpha\rangle\Big)_{\Phi_n}|\beta\rangle &= |\alpha\beta\rangle - |\Phi\rangle\langle\Phi|\alpha\beta\rangle, \\ \Big(\frac{\partial}{\partial|x\rangle}|\lambda_0\rangle\Big)_{\Phi_n}|\beta\rangle &= |0\beta\rangle + \sum_{\alpha=1}^{N_L}\Big((2|\alpha\rangle + |\Phi\rangle\langle\mathcal{L}_\alpha\rangle) \\ &\quad \times\langle\alpha|\beta\rangle - |\Phi\rangle\langle\Phi|\alpha\beta\rangle\Big\langle\mathcal{L}_\alpha^\dagger\Big\rangle\Big);\end{aligned}$$

the y-derivatives are

$$\begin{aligned}\langle\beta|\Big(\frac{\partial}{\partial\langle y|}|\lambda_\alpha\rangle\Big)_{\Phi_n} &= -|\Phi\rangle\langle\beta|\alpha\rangle, \\ \langle\beta|\Big(\frac{\partial}{\partial\langle y|}|\lambda_0\rangle\Big)_{\Phi_n} &= \Big((|\alpha\rangle 2 + |\Phi\rangle\langle\mathcal{L}_\alpha\rangle)\langle\beta\alpha|\Phi\rangle - |\Phi\rangle\langle\beta|\alpha\rangle\Big\langle\mathcal{L}_\alpha^\dagger\Big\rangle\Big);\end{aligned}$$

and the mixed derivatives are

$$\langle\alpha|\Big(\frac{\partial^2}{\partial|x\rangle\partial\langle y|}|\lambda_{\alpha'}\rangle\Big)_{\Phi_n}|\alpha\rangle = -\big(|\alpha\rangle\langle\alpha|\alpha'\rangle + |\Phi\rangle\langle\alpha|\alpha'\alpha\rangle\big),$$

$$\begin{aligned}&\langle\alpha|\Big(\frac{\partial^2}{\partial|x\rangle\partial\langle y|}|\lambda_0\rangle\Big)_{\Phi_n}|\alpha\rangle \\ &\quad = |\alpha\rangle\Big(2\langle\alpha'\alpha|\alpha'\rangle + \langle\mathcal{L}_{\alpha'}\rangle\langle\alpha'\alpha|\Phi\rangle - \langle\alpha'|\alpha\rangle\Big\langle\mathcal{L}_{\alpha'}^\dagger\Big\rangle\Big) \\ &\qquad + 2|\alpha'\alpha\rangle\langle\alpha\alpha'|\Phi\rangle - |\Phi\rangle\Big(\big|\langle\alpha|\alpha'\rangle\big|^2 + \big|\langle 0|\alpha'\alpha\rangle\big|^2 \\ &\qquad + 2i\Im\big[\langle\alpha\alpha'|\alpha\rangle\langle\mathcal{L}_{\alpha'}\rangle\big]\Big).\end{aligned}$$

A further simplification is obtained using the following summed kets:

$$\begin{aligned}&|e^0\rangle \equiv I^{0\alpha}|\alpha\rangle, \quad |f^0\rangle \equiv I^{\alpha 0}|\alpha\rangle, \quad |f^{0*}\rangle \equiv I^{\alpha 0*}|\alpha\rangle, \\ &|c\rangle \equiv c^\alpha|\alpha\rangle, \quad |d\rangle \equiv d^\alpha|\alpha\rangle, \quad |d^*\rangle \equiv d^{\alpha*}|\alpha\rangle, \quad |dc\rangle \equiv d^{\alpha'}\Lambda_{\alpha'}|c\rangle,\end{aligned}$$

with which the $'X'$, $'Y'$, and $'XY'$ terms of Eq. (12) become

$$\begin{aligned}'X' = {} & \frac{\Delta T^2}{2}\Big(|00\rangle + \Big((2|\alpha\rangle + |\Phi\rangle\langle\mathcal{L}_\alpha\rangle)\langle\alpha|0\rangle - |\Phi\rangle\langle\Phi|\alpha 0\rangle\Big\langle\mathcal{L}_\alpha^\dagger\Big\rangle\Big) \\ & + |0f^0\rangle + |e^0 0\rangle + \Big((2|\alpha\rangle + |\Phi\rangle\langle\mathcal{L}_\alpha\rangle)\langle\alpha|f^0\rangle \\ & - |\Phi\rangle\langle\Phi|\alpha f^0\rangle\Big\langle\mathcal{L}_\alpha^\dagger\Big\rangle\Big) - |\Phi\rangle\langle\Phi|e^0 0\rangle + |dc\rangle - |\Phi\rangle\langle\Phi|dc\rangle,\end{aligned}$$

$$\begin{aligned}'Y' = {} & \frac{\Delta T^2}{2}\Big((|\alpha\rangle 2 + |\Phi\rangle\langle\mathcal{L}_\alpha\rangle)\langle 0\alpha|\Phi\rangle - |\Phi\rangle\langle 0|\alpha\rangle\Big\langle\mathcal{L}_\alpha^\dagger\Big\rangle\Big) \\ & + \Big[\big(|\alpha'\rangle 2 + |\Phi\rangle\langle\mathcal{L}_{\alpha'}\rangle\big)\langle f^{0*}\alpha'|\Phi\rangle - |\Phi\rangle\Big\langle f^{0*}|\alpha'\rangle\Big\langle\mathcal{L}_{\alpha'}^\dagger\Big\rangle\Big] \\ & - |\Phi\rangle\langle 0|e^0\rangle - |\Phi\rangle\langle d^*|c\rangle,\end{aligned}$$

$$\begin{aligned}'XY' = {} & -2\big(|\alpha\rangle\langle\alpha|e^0\rangle + |\Phi\rangle\langle\alpha|e^0\alpha\rangle\big) \\ & + |\alpha\rangle\Big(2\langle\alpha'\alpha|\alpha'\rangle + \langle\mathcal{L}_{\alpha'}\rangle\langle\alpha'\alpha|\Phi\rangle - \langle\alpha'|\alpha\rangle\Big\langle\mathcal{L}_{\alpha'}^\dagger\Big\rangle\Big)\Delta T^2 \\ & + |\alpha'\alpha\rangle\big(2\langle\alpha\alpha'|\Phi\rangle\big)\Delta T^2 - |\Phi\rangle\Big(\big|\langle\alpha|\alpha'\rangle\big|^2 + \big|\langle 0|\alpha'\alpha\rangle\big|^2 \\ & + 2i\Im\big[\langle\alpha\alpha'|\alpha\rangle\langle\mathcal{L}_{\alpha'}\rangle\big]\Big)\Delta T^2.\end{aligned} \tag{13}$$

This completes the description of the method. As for the algorithmic scaling in N_L, the evaluation of each of the terms in the "X" and "Y" expressions requires order N_L operations (linear scaling effort in the number of Lindblad operators). However, the "XY" expression includes terms that require order N_L^2 operations, which may dominate the calculation as N_L grows.

After each time step is completed, we update the time $t_n \to t_{n+1} = t_n + \Delta T$ and the operators $\mathcal{L}_\alpha \to e^{i\mathcal{H}_0\Delta T}\mathcal{L}_\alpha e^{-i\mathcal{H}_0\Delta T}$ ($\alpha = 1,\ldots,N_L$) and $\mathcal{V}_0 \to e^{i\mathcal{H}_0\Delta T}\mathcal{V}_0 e^{-i\mathcal{H}_0\Delta T}$. Using the new value of $\mathcal{L}_\alpha$ and Φ, we calculate Λ_β ($\beta = 0,\ldots,N_L$) in preparation for the next time-step.

We set up the calculation in the following way: first, we define a macro-time state $\tau = N\Delta T$. We propagate from $\Phi^0 = \Psi(0)$ with N steps of ΔT, reaching Φ^N, and then, we transform back to the Schrödinger picture,

$$\Psi^N = e^{-i\mathcal{H}_0\tau}\Phi^N.$$

It is worth mentioning that our algorithm covers, as a special case, the *linear unraveling procedure*,[6,32]

$$|d\psi\rangle = -i\Big(\mathcal{H}_0 + \theta(t)\,\mathcal{V}_0(t) - i\mathcal{L}_\alpha^\dagger\mathcal{L}_\alpha\Big)|\psi\rangle dt + \mathcal{L}_\alpha|\psi\rangle d\omega^\alpha, \quad (14)$$

which is obtained from Eq. (3) by setting $\langle\mathcal{L}_\alpha\rangle \to 0$. Indeed, one can use the algorithm above and simplify by replacing Λ_α by $\mathcal{L}_\alpha$ and "X" by $\frac{\Delta T^2}{2}|00\rangle + |dc\rangle$ and by setting both "Y" and "XY" to zero in Eq. (12).

III. VALIDATION: MORSE OSCILLATOR

The example for our method is a Morse oscillator coupled to the environment at inverse temperature β_e. The particle has mass $m = 1$, and the truncated Morse potential is $U(x) = \max\left[U_{\max}, V_\infty\left(1 - e^{-ax}\right)^2\right]$ (see Fig. 1), with $V_\infty = 4$, $a = 0.2$, and $U_{\max} = 6$. As before, we use atomic units a_0 (Bohr radius) for lengths, E_h (Hartree energy) for energy, m_e (electron mass) for mass, and $\hbar E_h^{-1}$ for time. The wave functions $\psi(x)$ we consider here may have non-zero values only in the interval $x \in [-10, 30]$. We represent the system on a 31-point grid of unit spacing ($\Delta x = 1$),

$$x_n = -10 + n\Delta x, \quad n = 0, \ldots, 30. \quad (15)$$

The wave functions map into the vectors $\psi_n = \psi(x_n)$. The position ($\mathcal{X}$) and potential $\mathcal{U}_0 \equiv U(\mathcal{X})$ operators operate as $(\mathcal{X}\psi)_n = x_n\psi_n$ and $(\mathcal{U}_0\psi)_n = U(x_n)\psi_n$, respectively. The kinetic energy operator is the finite difference operator $(\mathcal{K}_0\psi)_n = -\frac{\hbar^2}{2m\Delta x^2}(\psi_{n-1} - 2\psi_n + \psi_{n+1})$, combined with the boundary condition $\psi_{-1} \equiv \psi_{31} \equiv 0$. This defines the Hamiltonian $\mathcal{H}_0 = \mathcal{K}_0 + \mathcal{U}_0$. The lowest lying bound energy levels of this Hamiltonian, determined by diagonalization, are shown in Fig. 1.

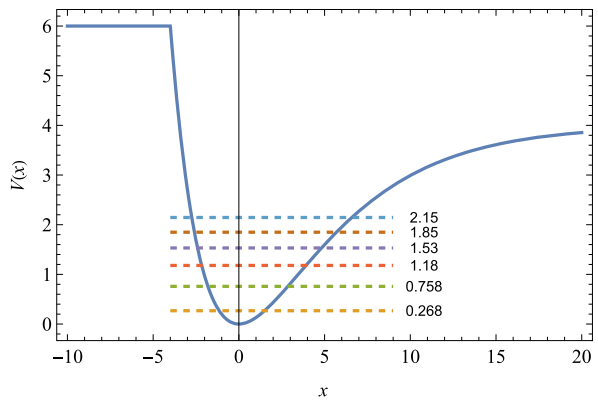

FIG. 1. Morse potential $U(x)$ used in this example. The dashed lines indicate the low lying energy eigenvalues.

We take only two Lindblad operators

$$\mathcal{L}_{\pm\omega_B,\mathcal{T}} = \sqrt{\gamma_{\pm\omega_B}} \times \frac{1}{2\mathcal{T}}\int_{-\mathcal{T}}^{\mathcal{T}} e^{\pm i\omega_B\tau}\,\mathcal{X}_H(\tau)d\tau, \quad (16)$$

where $\mathcal{X}_H(\tau) = e^{\frac{i}{\hbar}\mathcal{H}_0\tau}\mathcal{X}e^{-\frac{i}{\hbar}\mathcal{H}_0\tau}$ is the time-dependent Heisenberg operator for $\mathcal{X}$, $\mathcal{T} = 10$, and $\omega_B = \hbar^{-1}(E_1 - E_0) = \hbar^{-1} \times 0.4903$. The rates in Eq. (16) are chosen as

$$\gamma_{\pm\omega_B} = \frac{\gamma_0}{1 + e^{\pm\beta_e\hbar\omega_B}},$$

where $\gamma_0 = 0.2$ and the environment inverse temperature $\beta_e = 4$. These rates obey the detailed balance condition

$$\frac{\gamma_{\omega_B}}{\gamma_{-\omega_B}} = e^{-\beta_e\hbar\omega_B}. \quad (17)$$

The last element of the model problem is the initial state, which we take as a pure state $\rho(0) = |\xi\rangle\langle\xi|$:

$$|\xi\rangle = \frac{1}{\sqrt{3}}(|\psi_2\rangle + |\psi_3\rangle + |\psi_4\rangle), \quad (18)$$

where $|\psi_n\rangle$ are the eigenvectors of the Hamiltonian operator $\mathcal{H}_0$.

A. The "free" oscillator

We first discuss a time-independent case, where the oscillator is free, i.e., not subjected to an external driving force beyond the interaction with the environment. Using a small time step and a fourth-order Runge–Kutta propagator, we evolve the density operator according to the Lindblad equation [Eq. (1)], starting from $\rho(t = 0)$ and obtain highly accurate reference values for benchmarking the stochastic propagators. We find that the extended time limit of the evolved state is close, but not exactly equal, to the thermal state at the environmental temperature. In order to converge fully into the thermal state, we need to provide more Lindblad operators than just the two we consider here.

The stochastic calculation provides confidence intervals for the Lindblad expectation values $\mathrm{Tr}\,[\rho_t\mathcal{A}]$ of any given observable of interest $\mathcal{A}$. The procedure is a straightforward application of statistical analysis. We run our propagator N_s times (with independent random numbers) collecting N_s samples of quantum expectation values $A_t^{(k)} \equiv \left\langle\Psi_t^{(k)}|\mathcal{A}|\Psi_t^{(k)}\right\rangle / \left\langle\Psi_t^{(k)}\middle|\Psi_t^{(k)}\right\rangle$ $(k = 1, \ldots, N_s)$ and then construct the 95% confidence interval as $\left[\bar{A}_t - \Delta A_t, \bar{A}_t + \Delta A_t\right]$, where $\bar{A}_t$ is the sample average, $\Delta A_t = 2 \times S_t/\sqrt{N_s}$ is the interval width, and S_t is the sample standard deviation. The factor 2 is the large sample t-factor corresponding to a confidence level of ~95%. In Fig. 2, we show confidence intervals for two observables, the energy $\mathcal{H}_0$ and the position $\mathcal{X}$, using $N_s = 64$ and 1024 samples based on the first-order and second-order propagators with time step $\Delta T = 0.25$. For reference, the red solid line in the figure also shows the numerically exact expected value $\mathbb{E}[\langle\psi_t|\mathcal{A}|\psi_t\rangle] = \mathrm{Tr}\,[\rho_t\mathcal{A}]$.

The first-order calculation exhibits a noticeable energy bias at $\Delta T = 0.25$, even when the confidence interval is broad (when $N_s = 64$). At the same time, the bias from the second-order calculation is not noticeable even for the $N_s = 1024$ sampling. We discuss the weak order convergence comparing first-order and second-order methods below. The standard deviation S_t in the first-order and

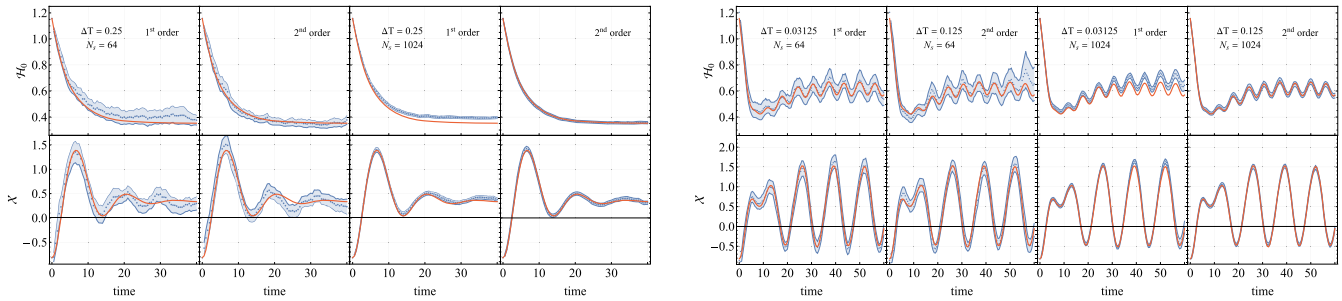

FIG. 2. The 95% confidence region (blue shade) for the energy (top panels) and position (bottom panels) transients of the free (left) and driven (right) Morse oscillator starting from a hot state, obtained from the first-order and second-order solutions of the ISE [Eqs. (9) and (12)] using $N_s = 64$ and 1024 samples. In addition the red lines show the numerically exact energy and the position transients calculated by solving Eq. (1).

second-order calculations is around 0.08 for the energy and 0.6 for the position; interestingly, it does not grow with time. We also checked the algorithm for the case of over-damped dynamics where a parameter of $\gamma = 0.6$ was used. We observed similar trends as in weak coupling in terms of the accuracy of the calculation (see details in the supplementary material). In terms of stability, both first-order and second-order calculations required time steps of at least 0.0625, and for larger time steps, the solution was unstable and diverged.

In a weak order-o method, $\mathbb{E}[\langle\Psi_t|\mathcal{A}|\Psi_t\rangle]$ should approach the exact value $\mathrm{Tr}\,[\rho_t\mathcal{A}]$ as the o power of ΔT. More precisely, there exist $\Delta T_0 > 0$ and $C > 0$ such that

$$\Delta T < \Delta T_0 \Rightarrow |\mathbb{E}[\langle\Psi_t|\mathcal{A}|\Psi_t\rangle] - \mathrm{Tr}\,[\rho_t\mathcal{A}]| \le C \times \Delta T^o. \tag{19}$$

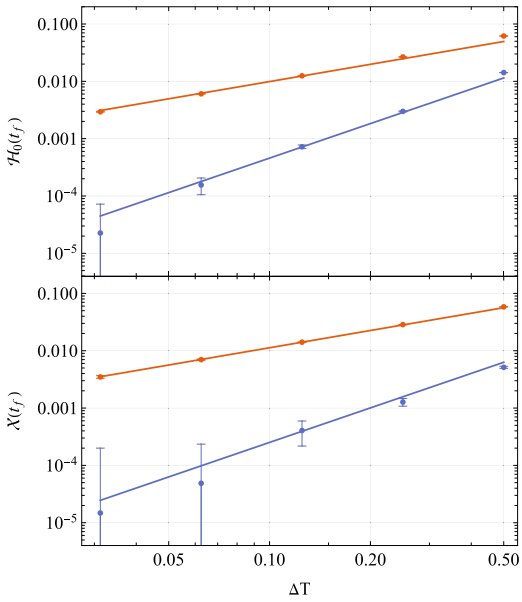

FIG. 3. Log-plots showing the first-order (red) and second-order (blue) confidence intervals for the energy $\mathcal{H}_0(t_f)$ (top panel) and position $\mathcal{X}(t_f)$ (bottom panel) expectation values at $t_f = 7$ vs time step ΔT. The dotted straight lines show asymptotic first-order and second-order behaviors [Eq. (19)]. The number of samples used for estimating the confidence intervals was $N_s = 64 \times 10^6$.

To test whether this condition is obeyed, we need to know $\mathbb{E}[\langle\Psi_t|\mathcal{A}|\Psi_t\rangle]$ and this is not available directly. However, we can build a very small 95% confidence interval by extensive sampling (taking $N_s = 64 \times 10^6$), as shown in Fig. 3, for the energy and position observables at time $t_f = 7$ as a function of the time step ΔT. The asymptotic behavior of Eq. (19) is clearly seen as the asymptotic lines do, indeed, fit through the very small confidence intervals. The power of the second-order calculations is also evident as its error with $\Delta T = 0.25$ is smaller than the error in the first-order calculation using a time step smaller by a factor of 8.

To assess the utility of the second-order vs the first-order solvers, we note that for the example given here, the wall-time for the former is only 1.5 times larger than the latter. This small ratio in wall times will characterize larger systems, as long as there is only one Lindblad operator. From the discussion above, concerning the time-step (and, hence, the number of time steps) required by both the methods, we conclude that in the present example, the second-order solver is five times more efficient than the first-order one for low-accuracy calculations. For higher accuracies, it is considerably more efficient. However, the wall time in the second-order calculation depends quadratically on the number N_L of Lindblad operators, while that of the first-order calculation is linear in N_L. Hence, the numerical cost of the second-order calculation may exceed that of the first-order calculation as N_L grows.

We mention briefly that linear unraveling [Eq. (14)] has a variance one to two orders of magnitude larger than for the nonlinear unraveling (and it grows linearly with time). Hence, the nonlinear unraveling is expected to be superior.

B. The driven oscillator

In this example, we subject the Morse oscillator to a driving time-dependent field,

$$\mathcal{V}_0\theta(t) = \mathcal{X}\mathcal{F}\,\sin(\omega t), \tag{20}$$

with $\mathcal{F} = 0.2$ and $\omega = 0.49$. The frequency is resonant between the ground and the first excited states of the oscillator. In Fig. 2 (right), we show first-order and second-order results for $N_s = 64$ and 1024 samples, respectively. The oscillator starts from the same pure state as in the example given in Sec. III A [see Eq. (18)]. Under the driving force, it strives to cool due to the interaction with the

cold environment but the driving field acts to heat it. Eventually, a quasi-stationary non-thermal state forms, with the oscillator energy and position oscillating strongly in time. The first-order solution is unstable for $\Delta T > 0.031\,25$, and even at this, a small time-step exhibits a large energy bias (red line not passing in the confidence interval for $N_s = 1024$). The second-order results are stable and much more accurate even when $\Delta T = 0.125$. As for the standard deviation S_t in the driven oscillator, it is around 0.25 for energy and 0.6 for position. As with the free oscillator, S_t does not grow with time.

IV. CONCLUSIONS

We have presented a weak second-order method for solving the Itô–Schrödinger equation related to quantum state diffusion unraveling of the Lindblad equation. One of the critical characteristics of the approach is working in the interaction picture, helping stability and accuracy even for relatively large time steps. Another significant characteristic of our approach is nonlinear unraveling, using the expectation value of the Lindblad operator within the equation, which reduces the variance (in comparison with the linear unraveling schemes). Moreover, the use of *explicitly normalized* expectation values of the Lindblad operators [Eq. (4)] further stabilizes the propagation. Another characteristic of our approach is using exact derivatives, which are readily available since our nonlinearity is analytical, for the Itô–Taylor expansion (as opposed to other second-order approaches, such as the Runge–Kutta method, which bypasses derivatives using finite difference). Finally, our method uses complex Wiener processes.

We have tested the method on the problem of cooling an initially hot Morse oscillator coupled to a colder environment. We studied both free and driven oscillators. In both cases, we showed a good accuracy of the second-order method when the time step was $\Delta T\omega_B \approx 0.1$ or smaller, achieving useful confidence intervals with a relatively small amount of sampling.

We have used 1D examples to benchmark our methods. For such small systems, unraveling does not save computational resources relative to a complete solution of the Lindblad equation. However, the latter method has cubic scaling in wall time and quadratic scaling in memory, and therefore, unraveling can become more efficient as systems grow. One clear advantage of unraveling is that it does not require storing the density matrix, saving a vast amount of computer memory. Furthermore, the most intensive part of the unraveling calculation, namely transforming to and from the interaction picture, can be accomplished by iterative methods[37,38] involving a fixed number of Hamiltonian applications to any given ket. As systems grow, this latter operation becomes linear-scaling in complexity, endowing the entire unraveling procedure with the same complexity. Thus, there is a massive reduction in computational time relative to a complete solution of the Lindblad equation in the limit of large systems. Furthermore, multiprocessor parallelization can easily overcome the burden of repeated sampling in the unraveling procedure.

The propagator developed in the present paper is our first step toward a more general goal of constructing a framework for studying quantum decoherence and dissipation in large molecular and nanoscale systems. The computational wall-time involved in the second-order calculation scales quadratically with the number N_L of Lindblad operators. Therefore, our immediate future work will involve a method to contract Lindblad operators so that a small, hopefully, system-size-independent number of operators can be used. In addition, in the future, we may try to develop solvers for stochastic Schrödinger equations that unravel non-Markovian master equations. Such solvers are required since the Markovian dynamics may result in unreliable predictions of bath-induced coherences.[39–42]

SUPPLEMENTARY MATERIAL

The supplementary material includes the derivation of Eq. (12) and the results of the Morse oscillator in the overdamped limit.

ACKNOWLEDGMENTS

The authors acknowledge the funding from the Israel Science Foundation under Grant No. ISF-800/19.

AUTHOR DECLARATIONS

Conflict of Interest

The authors have no conflicts to disclose.

Author Contributions

Sayak Adhikari: Conceptualization (supporting); Data curation (lead); Formal analysis (equal); Investigation (equal); Methodology (equal); Validation (equal); Visualization (equal); Writing – original draft (supporting); Writing – review & editing (supporting). **Roi Baer**: Conceptualization (lead); Data curation (supporting); Formal analysis (equal); Funding acquisition (lead); Investigation (equal); Methodology (equal); Project administration (lead); Software (equal); Supervision (lead); Validation (equal); Visualization (equal); Writing – original draft (lead); Writing – review & editing (lead).

DATA AVAILABILITY

The data that support the findings of this study are available within the article.

REFERENCES

[1] W. T. Pollard and R. A. Friesner, "Solution of the Redfield equation for the dissipative quantum dynamics of multilevel systems," J. Chem. Phys. **100**(7), 5054–5065 (1994).
[2] D. Kohen, C. C. Marston, and D. J. Tannor, "Phase space approach to theories of quantum dissipation," J. Chem. Phys. **107**(13), 5236–5253 (1997).
[3] A. Nitzan, *Chemical Dynamics in Condensed Phases: Relaxation, Transfer and Reactions in Condensed Molecular Systems*, *Oxford Graduate Texts* (Oxford University Press, Oxford, New York, 2006).
[4] U. Harbola, M. Esposito, and S. Mukamel, "Quantum master equation for electron transport through quantum dots and single molecules," Phys. Rev. B **74**(23), 235309 (2006).
[5] H.-P. Breuer and F. Petruccione, *The Theory of Open Quantum Systems* (Oxford University Press, 2007).
[6] H. Appel and M. Di Ventra, "Stochastic quantum molecular dynamics," Phys. Rev. B **80**(21), 212303 (2009).

[7]Á. Rivas and F. Susana Huelga, *Open Quantum Systems: An Introduction. Springer Briefs in Physics* (Springer, Heidelberg, 2012), OCLC: 759533862.
[8]R. Biele and R. D'Agosta, "A stochastic approach to open quantum systems," J. Phys.: Condens. Matter **24**(27), 273201 (2012).
[9]K. Blum, *Density Matrix Theory and Applications, of Springer Series on Atomic, Optical, and Plasma Physics* (Springer Berlin Heidelberg, Berlin Heidelberg, 2012), Vol. 64.
[10]G. Schaller, *Open Quantum Systems Far from Equilibrium* (Springer, 2014), Vol. 881.
[11]C. Gardiner and P. Zoller, *The Quantum World of Ultra-cold Atoms and Light Book I: Foundations of Quantum Optics* (World Scientific Publishing Company, 2014).
[12]R. Uzdin and R. Kosloff, "Speed limits in Liouville space for open quantum systems," Europhys. Lett. **115**(4), 40003 (2016).
[13]R. Alicki and R. Kosloff, "Introduction to quantum thermodynamics: History and prospects," in *Thermodynamics In the Quantum Regime, Volume 195 of Fundamental Theories of Physics*, 1st ed., edited by F. Binder, L. C. G. Correa, J. Anders and G. Adesso (Springer, Cham, 2018); arXiv:1801.08314.
[14]Z. Ruan and R. Baer, "Unravelling open-system quantum dynamics of non-interacting Fermions," Mol. Phys. **116**, 2490–2496 (2018).
[15]G. Kurizki and G. Abraham Kofman, *Thermodynamics and Control of Open Quantum Systems*, 1st ed. (Cambridge University Press, December, 2021).
[16]A. Levy, E. Rabani, and T. David, "Limmer. Response theory for nonequilibrium steady states of open quantum systems," Phys. Rev. Res. **3**, 2023252 (2021).
[17]M. Gerry and D. Segal, "Full counting statistics and coherences: Fluctuation symmetry in heat transport with the unified quantum master equation," Phys. Rev. E **107**(5), 054115 (2023).
[18]A. G. Redfield, "On the theory of relaxation processes," IBM J. Res. Dev. **1**(1), 19–31 (1957).
[19]P. Gaspard and M. Nagaoka, "Slippage of initial conditions for the Redfield master equation," J. Chem. Phys. **111**(13), 5668–5675 (1999).
[20]M. Esposito and M. Galperin, "Self-consistent quantum master equation approach to molecular transport," J. Phys. Chem. C **114**(48), 20362–20369 (2010).
[21]T. Becker, L.-N. Wu, and A. Eckardt, "Lindbladian approximation beyond ultraweak coupling," Phys. Rev. E **104**(1), 014110 (2021).
[22]G. Lindblad, "On the generators of quantum dynamical semigroups," Commun. Math. Phys. **48**(2), 119–130 (1976).
[23]V. Gorini, A. Kossakowski, and E. C. G. Sudarshan, "Completely positive dynamical semigroups of N -level systems," J. Math. Phys. **17**(5), 821–825 (1976).
[24]R. Alicki and K. Lendi, *Quantum Dynamical Semigroups and Applications*, *Volume 717 of Lecture Notes in Physics* (Springer, Berlin, Heidelberg, 2007).
[25]D. Manzano, "A short introduction to the Lindblad master equation," AIP Adv. **10**(2), 025106 (2020).
[26]M. B. Plenio and P. L. Knight, "The quantum-jump approach to dissipative dynamics in quantum optics," Rev. Mod. Phys. **70**, 101–144 (1998).
[27]I. Percival, *Quantum State Diffusion* (Cambridge University Press, 1998).
[28]J. Dalibard, Y. Castin, and K. Mølmer, "Wave-function approach to dissipative processes in quantum optics," Phys. Rev. Lett. **68**(5), 580–583 (1992).
[29]C. W. Gardiner, A. S. Parkins, and P. Zoller, "Wave-function quantum stochastic differential equations and quantum-jump simulation methods," Phys. Rev. A **46**(7), 4363–4381 (1992).
[30]C. Howard, *An Open Systems Approach to Quantum Optics: Lectures Presented at the Université Libre de Bruxelles* (Springer Science & Business Media, 1993), Vol. 18 October 28 to November 4, 1991.
[31]N. Gisin and I. C. Percival, "The quantum-state diffusion model applied to open systems," J. Phys., A Math. Gen. **25**(21), 5677–5691 (1992).
[32]J. Li and X. Li, "Exponential integrators for stochastic Schrödinger equations," Phys. Rev. E **101**(1), 013312 (2020).
[33]C. M. Mora and M. Muñoz, "On the rate of convergence of an exponential scheme for the non-linear stochastic Schrödinger equation with finite-dimensional state space," Phys. Scr. **98**(6), 065226 (2023).
[34]J. R. Johansson, P. D. Nation, and F. Nori, "QuTiP 2: A Python framework for the dynamics of open quantum systems," Comput. Phys. Commun. **184**(4), 1234–1240 (2013).
[35]E. PeterKloeden and E. Platen, *Numerical Solution of Stochastic Differential Equations* (Springer, 1992).
[36]G. N. Milstein, *Numerical Integration of Stochastic Differential Equations* (Springer, Netherlands, Dordrecht, 1995).
[37]M. Feit, J. A. Fleck, and A. Steiger, "Solution of the Schrödinger equation by a spectral method," J. Comput. Phys. **47**(3), 412–433 (1982).
[38]R. Kosloff, "Time-dependent quantum-mechanical methods for molecular dynamics," J. Phys. Chem. **92**(8), 2087–2100 (1988).
[39]M. Leijnse and M. R. Wegewijs, "Kinetic equations for transport through single-molecule transistors," Phys. Rev. B **78**(23), 235424 (2008).
[40]M. Esposito, M. A. Ochoa, and M. Galperin, "Efficiency fluctuations in quantum thermoelectric devices," Phys. Rev. B **91**(11), 115417 (2015).
[41]Y. Gao and M. Galperin, "Simulation of optical response functions in molecular junctions," J. Chem. Phys. **144**(24), 244106 (2016).
[42]L. Kidon, E. Y. Wilner, and E. Rabani, "Exact calculation of the time convolutionless master equation generator: Application to the nonequilibrium resonant level model," J. Chem. Phys. **143**(23), 234110 (2015).